May 16th, 2:55 PM

Experimental Investigation of Scour and Pressures on a Single Span Arch Bridge Under Inundation

Mohsen Ebrahimi
University of Exeter, m.ebrahimi@exeter.ac.uk

Recep Kahraman
University of Exeter

Matthew Riella
University of Exeter

Prakash Kripakaran
University of Exeter

Slobodan Djordjević
University of Exeter

See next page for additional authors

Recommended Citation

Ebrahimi, Mohsen (2018). Experimental Investigation of Scour and Pressures on a Single Span Arch Bridge Under Inundation. Daniel Bung, Blake Tullis, 7th IAHR International Symposium on Hydraulic Structures, Aachen, Germany, 15-18 May. doi: 10.15142/T33D25 (978-0-692-13277-7).

7th International Symposium on Hydraulic Structures Aachen, Germany, 15-18 May 2018
ISBN: 978-0-692-13277-7 DOI: 10.15142/T33D25

Experimental Investigation of Scour and Pressures on a Single Span Arch Bridge Under Inundation

M. Ebrahimi[1], R. Kahraman[1], M. Riella[1], P. Kripakaran[1], S. Djordjević[1], G. Tabor[1], D.M. Prodanović[2] & S. Arthur[3]
[1]*Centre for Water Systems, University of Exeter, Exeter, United Kingdom*
[2]*Faculty of Civil Engineering, University of Belgrade, Belgrade, Serbia*
[3]*Institute for Infrastructure and Environment, Heriot-Watt University, Edinburgh, United Kingdom*
E-mail: m.ebrahimi@exeter.ac.uk

Abstract: *This paper presents two experiments, carried out in a 605mm-wide flume, to investigate scour and hydrodynamic pressure on a scaled model of a single span arch bridge. The geometry of the bridge model is scaled down according to a prototype bridge, with hydraulic conditions of the experiments representing a small river. Measurements showed that vertical-contraction scour by the arch bridge is higher than that of flat-deck bridges. Effect of a single cylindrical debris on scour was also evaluated and found to be negligible at the considered flow depth. Temporal variation of hydrodynamic pressure with scour evolution was also measured. It was found that temporal evolution of scour can reduce hydrodynamic pressure significantly at the initial base of the abutment at downstream face of the bridge, which can erode mortar from the masonry composition of an arch bridge.*

Keywords: *Arch bridge, flume experiment, scour, pressure-flow, hydrodynamic pressure*

1. Introduction

Arch bridges form a major portion of bridges in the UK and Europe (Melbourne et al. 2007; Robinson 2000; Oliveira et al. 2010; Sarhosis et al. 2016). A large number of these structures, particularly those built before 19th century, are masonry structures. These constitute 40% of the UK bridge stock (McKibbins et al. 2006), and are classified as cultural and engineering heritage structures.

Arch bridges have been extensively studied for their structural stability under various scenarios such as vehicle impact, settlement of a pier due to scour and debris flow impact (Hobbs et al. 1998; Invernizz et al. 2011; Proske et al. 2017). To the best knowledge of authors, however, there is no literature record on hydrodynamic pressure at arch bridges. This is particularly true with a river bed experiencing scour in which variation of pressure with bed deformation may affect the masonry composition of the arch bridge. Scour can also endanger stability of the foundations and the bridge. While many factors can contribute to the failure of a bridge, scour is widely recognised as the leading cause (Chang 1973; HR Wallingford et al. 1991; Richardson et al. 1993; Parola et al. 1997; Melville and Coleman 2000; May et al. 2002; Hunt 2009; Ettema et al. 2010; Highways Agency 2012; Benn 2013; Toth 2015). Several recent examples highlight this aspect in the UK and abroad: Bridge RDG1 48 in 2009 near Feltham in England, Malahide Viaduct in Ireland in 2009, CPR Bonnybrook Bridge in 2013 in Calgary in Canada, I-10 Bridge in California, US in 2015, and several bridge failures in December 2015 in the Cumbria floods in the UK. In particular bridge abutment, scour is a significant cause of bridge failure (Sutherland 1986; Melville 1992).

Arch bridges have excellent vertical load bearing (Gibbons and Fanning 2012; Proske and van Gelder 2009); however, due to their typically short spans, low clearance and wide piers, they tend to cause a much larger obstruction to flow compared to modern bridges (Hamill 1998; McKibbins et al. 2006). Therefore, their scour depth can be higher than that of modern bridges. Also, due to the aforementioned properties, arch bridges are susceptible to issues such as debris blockage which can exacerbate scour. The present paper, via flume experiments, aims at studying scour depth at a single span arch bridge and also measuring temporal variation of hydrodynamic pressure at the abutments during scour evolution. In addition, effect of a simple cylindrical debris on scour is investigated.

The paper presents results from clear-water scour experiments in a flume containing a scale model of a small single span arch bridge with flow angle of attack relative to the bridge being zero. Considered flow was relatively deep with its free surface being above the bridge intrados (inner curve of the arch). The abutments of the bridge were flush to the vertical side walls of the flume; so, the setup is representative of a narrow river with very steep or nearly vertical banks.

2. Experimental Setup

Experiments were carried out in a horizontal sediment recirculating flume with the width B = 605 mm and working length of 10 m at the University of Exeter, UK. In total, two clear-water scour experiments (sand median grain size d_{50} = 1.37 mm and flow intensity U/U_{cr} = 0.86 where U_{cr} = critical flow velocity for initiation of sediment movement and U = mean velocity of approach flow) were carried out with identical flow depth and discharge. The second experiment used a cylindrical object under the flow free surface representing a large tree trunk being stuck at the bridge just under the free surface of the approach flow. This was carried out to investigate effect of a large tree trunk on scour and hydrodynamic pressure at the present deep flow. Considering the flume's relatively small width, experiments were designed to represent a short span bridge with prototype span length 5.56 m. Accordingly, the geometric scaling ratio of $\simeq$ 1/11 was chosen to design the bridge model. Uniform sand was used as bed material which would represent medium gravel in prototype scale. The surfaces of the bridge model were smooth, and any surface roughness of the masonry structure is disregarded.

2.1. Hydraulic Conditions of the Experiments

Hydraulic conditions of the experiments are presented in Table 1. B and h = width and depth of approach flow; Q = flow discharge; R = flow Reynolds number (= Uh/ν, with $U = Q/(Bh)$ and ν being mean velocity of approach flow and fluid kinematic viscosity, respectively); F = Froude number (= $U/(gh)^{1/2}$, where g is acceleration due to gravity); R_* = roughness Reynolds number = $u_* k_s/\nu$, with u_* = shear velocity calculated as proposed by Sheppard et al. (2014) and k_s = granular roughness = $2d_{50}$ (Kamphuis 1974); d_s = maximum scour depth.

Flow depth and discharge were identical in experiments 1 and 2. This was ensured by adjusting carefully the approach flow depth and discharge to be within 0.5 mm and 0.1 L/s, respectively, from the target value, as also stated in the Table 1. Approach flow depth was identified with h = 220 mm reaching above the bridge arch (see Fig. 1). Reynolds number scaling was relaxed while keeping R in the range of turbulent flow (Chanson 2004) and the approach flow was also kept subcritical (F < 1) rather than having strict Froude similitude between the model and prototype conditions. In both tests, the flow is uniform and in fully rough regime of turbulent flow (R_* > 70, Yalin and da Silva 2001).

Table 1. Hydraulic conditions experiments (d_{50} = 1.37 mm and B = 605 mm)

Experiment	Approach flow depth $h \pm 0.5$ (mm)	Flow discharge $Q \pm 0.1$ (L/s)	R	F	R_*	Debris status	Mean[a] maximum scour depth $d_s \pm 1$ mm
1	220	53.9	89091	0.28	76.6	No debris	161.3
2						Cylindrical	169.7

[a] over the two abutments

2.2. Bridge model

The overall geometry of the bridge model was based on the single span Canns Mill Bridge in Devon, UK (Devon County Council, private communication, 2015-2017). This bridge has very long abutments (in spanwise y direction) and the width of the flume would not allow for scaling these to the ratio 1:11. Therefore, bridge arch and vertical dimensions were scaled strictly, and the lateral length of the model was limited to 605 mm as shown in Fig. 1. This resulted in $L/h \simeq 0.24$ (where L = 52 mm is abutment length in y direction), while in prototype scale $L/h \sim 1.1$ for corresponding flow depth. In addition, the inclined banks of the river, being sloped at about 57 degrees, are replaced here with vertical side walls of the flume which may significantly affect the results. This was, however, neglected as the aim was to investigate overall scour depth and hydrodynamic pressure during temporal evolution of scour rather than having a realistic scenario. Also, due to practical restrictions, streamwise length (along x) of the bridge was limited to 362 mm while scale 1:11 would dictate 462 mm. The model was fabricated out of acrylic sheets with a hollow interior to allow for embedding pressure transducers. During each experiment, the upper part of the bridge (shown by hatched region in Fig. 1) was fixed to the lower legs of the bridge (shown by dashed lines) which were fixed to the flume base. For scour measurements after completing each experiment, the upper part was removed (Subsection 3.1).

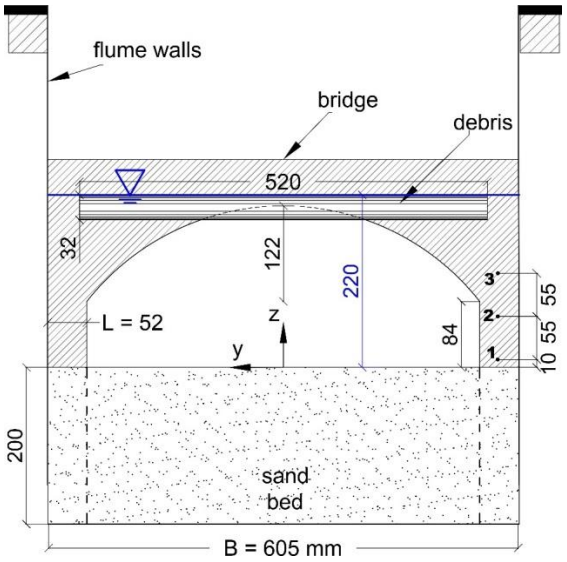

Figure 1. Looking-downstream cross-sectional schematic of experiment 2. The origin and orientation of the coordinate system used to discuss results is also shown. All dimensions are in mm and model length in streamwise *x* direction was 362 mm. Pressure transducers (3 sensors upstream and 3 sensors downstream) are numbered 1-3.

2.3. Sand and Scour

In the present work, sediment was coarse, uniform silica sand with particle size d_{50} and uniformity coefficient d_{60}/d_{10} equal to 1.37 mm and 1.37 respectively. This choice was determined by having 1) clear-water scour (with U/U_{cr} = 0.86 where U_{cr} = critical flow velocity for initiation of sediment movement, calculated as $U_{cr} = U/\eta_*^{1/2}$, where η_* is relative flow intensity calculated according to Yalin and da Silva (2001); 2) rough turbulent flow (R_* > 70, Yalin 1972) and 3) non-ripple forming sand (d_{50} > 0.6-0.7 mm, Raudkivi and Ettema 1983; Ettema et al. 1998) facilitating measurements of scour depth. d_{50} = 1.37 mm is representing medium gravel when scaled by 1:11 to the prototype scale.

Each scour experiment lasted 300 minutes. This is equivalent to $5\times11^{0.5}$ = 16.5 hours in prototype scale which is an already long event. This duration is, however, not sufficient for reaching equilibrium scour as it results in the scour depth reaching about 81% of equilibrium scour depth for a circular pier with diameter 52 mm and U/U_{cr} = 0.86 according to Melville and Chiew (1999).

2.4. Debris

As illustrated in Fig. 1, the effect on scour of a 32mm cylindrical debris fixed upstream the bridge just under the free surface of the approach flow was investigated in experiment 2. Therefore, accumulation of a matrix of smaller elements was not considered here. Instead, a simple cylindrical object was assumed to be transported to and stuck at the bridge and under free surface to represent a large tree trunk initiating debris accumulation and blocking the bridge opening partially. Therefore, the actual process of debris accumulation (e.g. Lyn et al. 2003; Panici and de Almeida 2017) and dynamics was not investigated. Instead, debris was considered to remain fixed at a certain position. The present debris model was solid and smooth. This is sufficient for the purposes of this study since as found by Pagliara and Carnacina (2010) and Lagasse et al. (2010) roughness of debris do not affect depth and pattern of scour in any appreciable way and can only be considered secondary factors when compared with dimensions of debris and flow intensity. Debris elevation, i.e. under the free surface, was chosen since yet unpublished experiments showed a cylindrical debris would cause highest increase of scour at this elevation compared to debris being at lower height from the bed.

3. Measurement Techniques

A 3-axis traverse system was utilised for positioning instruments at predefined (*x*, *y*, *z*) coordinates, with *x*, *y* and *z* being streamwise, spanwise and vertical directions. Experiments were started with a flat bed, with z = 0 representing bed level at t = 0. Flow discharge was set via a variable-speed drive and measured using an electromagnetic flowmeter (resolution ±0.1 L/s) installed in the suction pipe of the water recirculating system. Approach flow depth was measured using a digital point gauge mounted 3.5 m upstream the bridge to read undisturbed elevation of free surface. Due to free surface fluctuations, the point gauge precision in practice was 0.5 mm.

3.1. Scour

Final scour topography was measured after running each experiment for 300 minutes and stopping the flow gradually. This was carried out after removing the upper part of the bridge by measuring distances from the bed on a grid of approximately 230 (x, y) points using an echo-sounder with accuracy of 0.5 mm. Scour depths at around the bridge abutments that could not be easily reached using the echo-sounder were measured manually using a point gauge with precision of 0.5 mm. The final map of scour (Fig. 2), with expected accuracy of ±1 mm, was produced by combining all the measured points.

3.2. Hydrodynamic Pressure

Hydrodynamic pressure was measured at three points on the right (Fig. 1) abutments of the bridge model at upstream and downstream faces. This was carried out with sampling rate ~1 Hz using six pressure transducers (Honeywell 26PC series) with range 1 psi (6894.76 Pa) and accuracy in practice 3×10^{-4} psi (~ 2.1 Pa).

4. Results and Discussion

4.1. Scour

3D maps of scour measured after 300 minutes are shown in Fig. 2. Red and green shades show erosion and deposition respectively. At each abutment maximum scour depth was located at the front corner of the abutment. Ultimate maximum scour depth was located at the right abutment marked by a red line at about x = 0 and y = -52 mm. As can be seen, scour maps are fairly symmetrical about the x-z plane. However, there were some differences: scour depths d_s on each side of the flume at right and left abutments at experiment 1 were 168.6 and 154 mm (mean d_s = 161.3 mm), and at experiment 2 were 170.6 and 168.8 mm (mean d_s = 169.7 mm) respectively. Also, deposition of sand at green region downstream the bridge is not quite symmetrical about the x-z plane.

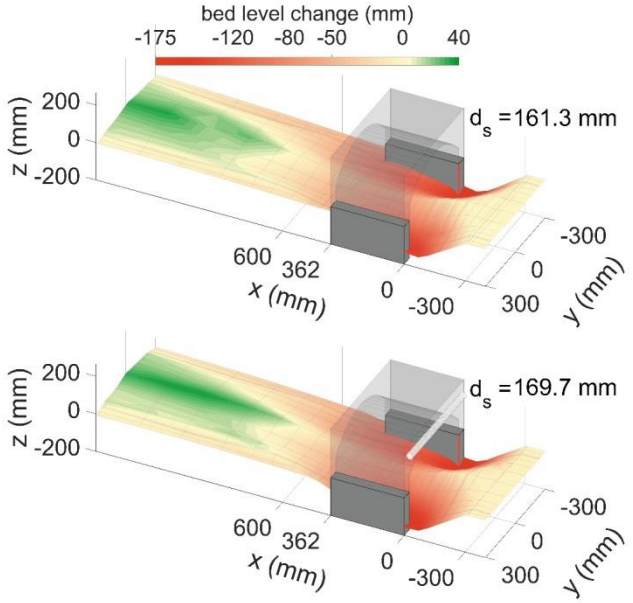

Figure 2. 3D maps of scour at experiments 1 (top) and 2 (bottom). Red line marks location of maximum depth of scour located at the abutment corner. The upper part of the bridge and the cylindrical debris are shown transparent.

At present setup, water surface elevation was above the bridge arch (intrados). This caused "orifice flow" with accelerated and directed-downward flow, and enhanced sediment transport capacity due to "pressure-flow scour" caused by vertical (along z) contraction (e.g. Abed 1991; Umbrell et al. 1998; Melville 2014; Kumcu 2016) due to the bridge arch. This is in addition to "contraction scour" caused due to lateral contraction by bridges abutments (Melville 1992).

It is known that pressure-flow would increase d_s by a factor of 2-4 depending on the Froude number and the size of the bridge opening (Abed 1991). Three well-known equations were used to estimate pressure-flow equilibrium scour depth at U/U_{cr} = 0.86, i.e. equations by Umbrell et al. (1998), Lyn (2006, who proposed a revised version of HEC-18 equation by Richardson and Davies 2001) and Melville (2014). Based on the results (Table 2), the equation by Melville (2014), giving the highest (most conservative) pressure-flow scour depth, is adopted.

Table 2. Pressure-flow equilibrium scour depth at threshold conditions estimated from three equations

Equation	d_s (mm)
Umbrell et al. (1998)	15
Lyn (2006)	14.7
Melville (2014)	75.6

Contraction equilibrium scour depth due to abutments using Melville (1992 and 1997) equation is 86.3 mm for U/U_{cr} = 0.86 and abutments with $L/h \simeq 0.24$. This results in total equilibrium scour depth (pressure-flow scour in Table 2 + abutment contraction scour) to be 161.9 mm. This is close to mean d_s = 161.3 mm observed at experiment 1 after 300 minutes. This may imply that at the present high flow depth causing pressure-flow and vertical contraction, scour depth at an arch bridge can be higher than that of flat-deck bridges. This can be due to the fact that available equations for estimating pressure-flow scour are developed based on flat-deck type bridges, while the present bridge model is an arch bridge which causes higher larger vertical blockage and contraction. It is, however, important to note that scour depth in the present flume experiments can be excessively large if scaled up to prototype scale with similar conditions. This is mainly due to inclined and rough banks with over bank flows in the field (Melville 1992), which were absent in the present setup.

Scour increase, after 300 minutes, due to cylindrical debris in experiment 2 was only about 5% higher than that of experiment 1. This is not surprising considering that the percentage of blockage by cylindrical debris relative to the original bridge opening was only 1.95% at the beginning of the experiment. This is in agreement with Pagliara and Carnacina (2011) in which small blockage area was found to cause very small increase of scour depth. Fig. 3 shows the present result combined with yet unpublished data of similar experiments with a sharp nose single pier being 50 mm wide. $d_{s,0}$ is the maximum scour depth at experiment without debris and d_s is maximum scour depth in corresponding experiment with 32mm cylindrical debris being just under water surface. As can be seen, as the flow becomes shallower (smaller h/L), $d_s/d_{s,0}$ increases and for deep flow with h/L >~ 4, debris effect is negligible and $d_s/d_{s,0}$ = 1. However, it should be noted that these results are valid only for 32mm cylindrical debris used here, and larger debris dimensions can cause high scour increase as shown by Pagliara and Carnacina (2011).

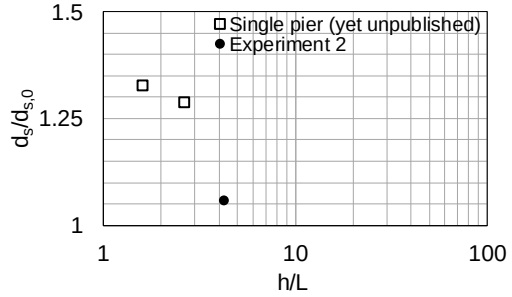

Figure 3. d_s increase due to 32mm cylindrical debris versus flow shallowness (flow depth h relative to pier width or abutment length L)

4.2. Hydrodynamic Pressure

Fig. 4 shows typical variation with time of measured total hydrodynamic pressure and its dynamic component. Pressures are normalised with respect to the corresponding initial (t = 0) hydrostatic pressure at each point (see Fig. 1). The patterns were similar for both experiments (with and without the cylindrical debris) and no meaningful difference was observed between the two tests; therefore, results from only one of the experiments are shown.

Total hydrodynamic pressure P is decomposed to static P_{st} and dynamic P_{dyn} components. At the beginning of each experiment, i.e. stagnant flow condition at t = 0, pressures are P_{dyn} = 0, $P = P_{st} = \gamma.h$ and P/P_{st} = 1. Preliminary experiments on fix bed without sand, showed that after starting the pump at t = 0 and bringing flow discharge to the target value, it takes about 97 seconds for the flow to reach fully developed state. This state is defined as free surface slope reaching a constant value and is mainly a characteristic of the pump recirculation system. Although in the present experiments with rough bed and scour, the equilibrium time can be different, 97 seconds is used as a guide to show variation of flow state during the early stages of the experiment. This is shown by dotted line in Figure 4. Starting the flow caused hydrodynamic pressure and also total pressure at downstream points DS1, DS2 and DS3 to drop considerably. The reduction in P_{dyn} is attributed to the local presence of vortices and flow separation caused by the bridge behaving as a step to the flow pathway. This is more severe at point DS1 near the initial base of abutments (Baker 1979 and 1980) while at higher elevations at points DS2 and DS3 smaller pressure

drop is observed. At upstream face at points US2 and US3, there is small increase in P_{dyn} which could be due to the absence or low severity of vortices (Breusers et al. 1977; Richardson and Panchang 1998) and higher flow momentum. After flow development (at $t \simeq 0.027$ hour = 97 seconds) it takes about 13 and 37 minutes for the P_{dyn} to reach the local minimum or maximum at US1 and DS1 respectively. This implies a rather long transition process in the flow to reach an equilibrium condition with scour evolution which is responsible for changing flow momentum and thereby dynamic and total pressure (it is also worthwhile to note that P_{st} has small contribution in variation of total pressure due to rising and dropping water free surface, at upstream and downstream faces respectively, with starting the flow at $t = 0$. This was neglected in above analysis).

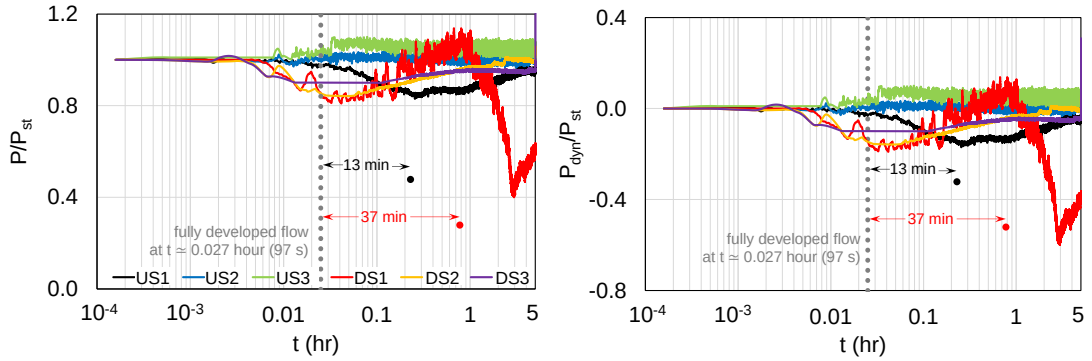

Figure 4. Typical temporal variation with time of normalised (with respect to P_{st} at each point at $t = 0$) pressures at points 1, 2 and 3 (Fig. 1) at upstream (US) and downstream (DS) faces: (left) total pressure; (right) dynamic pressure.

From Fig. 4 it can be inferred that during the present 5-hour experiments, P_{dyn} was either negligible or reducing total pressure at each point. At points US1, DS2 and DS3, in spite of pressure drop at early stages of the experiment, pressure seems to increase back to pressure at $t = 0$ as scour hole became deeper with time. At point DS1 it is, however, difficult to predict the variation of pressure after 5 hours; negative P_{dyn} could become even larger and reduce total pressure below zero. Negative total pressure (suction) can then erode the mortar from the masonry structure of the bridge and affect its structural integrity. Whether pressure increases or decreases after 5 hours has to be investigated with long duration experiments or simulations.

5. Conclusions

Main findings from the present work are as follows.

1. For the tested model of a single span arch bridge, measured scour depth after 5 hours was close to the equilibrium scour depth estimated by available empirical equations for flat-deck bridges. This can imply that at an inundated arch, scour rate is much higher than that of a flat-deck bridge.. This is due to the vertical contraction and pressure-flow caused by the arch.
2. For debris dimension and flow depth at present work, the effect of debris on scour depth was negligible. This was related to the small blockage ratio in deep flow. In shallower flows, same debris, however, can cause significant increase in scour depth (Figure 3).
3. The most critical location, in terms of hydrodynamic pressure at the bridge abutments of a single span arch bridge is near the initially flat bed and at downstream side of the bridge. At this point, total pressure may become negative and affect structural integrity by eroding the mortar from masonry composition of the arch bridge.

6. Acknowledgements

The research presented in this paper was supported by funding from the UK's Engineering and Physical Sciences Research Council (EPSRC) under grant EP/M017354/1. The authors are grateful to all project partners for their support, particularly Devon County Council, for providing useful prototype data. Data supporting the presented work can be accesses via authors or contacting University of Exeter's repository ORE. For further information please refer to the project blog at http://blogs.exeter.ac.uk/ramb/

7. References

Abed, L. M. (1991). “Local scour around bridge piers in pressure flow.” Colorado State University.

Baker, C. J. (1979). “The laminar horseshoe vortex.” *Journal of Fluid Mechanics*, 95(2), 347–367.

Baker, C. J. (1980). “The turbulent horseshoe vortex.” *Journal of Wind Engineering and Industrial Aerodynamics*, 6(1), 9–23.

Benn, J. (2013). “Railway bridge failure during flooding in the UK and Ireland.” *Proceedings of the Institution of Civil Engineers - Forensic Engineering*, 166(4), 163–170.

Breusers, H. N. C., Nicollet, G., and Shen, H. W. (1977). “Local Scour Around Cylindrical Piers.” *Journal of Hydraulic Research*, 15(3), 211–252.

Chang, F. F. M. (1973). *A statistical summary of the cause and cost of bridge failures*.

Chanson, H. (2004). *The hydraulics of open channel flow: basic principles, sediment motion, hydraulic modelling, design of hydraulic structures*. Elsevier [u.a.], Amsterdam.

Ettema, R., Melville, B. W., and Barkdoll, B. (1998). “Scale Effect in Pier-Scour Experiments.” *Journal of Hydraulic Engineering*, 124(6), 639–642.

Ettema, R., Nakato, T., and Muste, M. (2010). *Estimation of scour depth at bridge abutments*. National Cooperative Highway Research Program.

Gibbons, N., and Fanning, P. J. (2012). “Rationalising assessment approaches for masonry arch bridges.” *Proceedings of the Institution of Civil Engineers - Bridge Engineering*, 165(3), 169–184.

Hamill, L. (1998). *Bridge Hydraulics*. CRC Press.

Highways Agency. (2012). *The assessment of scour and other hydraulic actions at highway structures.* U.K.

Hobbs, B., Gilbert, M., and Molyneaux, T. (1998). “Effects of vehicle impact loading on masonry arch parapets.” *Arch bridges: history, analysis, assessment, maintenance and repair. Proceedings of the Second International Arch Bridge Conference*.

HR Wallingford, O’Sullivan, T. P., and & Partners. (1991). *Hydraulics of highway structures. Report EX2404 Part 1*. Contract report for Transport and Road Research Labor-atory.

Hunt, B. E. (2009). *Monitoring Scour Critical Bridges*. Transportation Research Board, Washington, D.C.

Invernizz, S., Lacidogna, G., Manuello, A., and Carpinteri, A. (2011). “AE Monitoring and Numerical Simulation of a Two-span Model Masonry Arch Bridge Subjected to Pier Scour.” *Strain*, 47(Suppl. 2), 158–169.

Kamphuis, J. W. (1974). “Determination of sand roughness for fixed beds.” *Journal of Hydraulic Research*, 12(2), 193–203.

Kumcu, S. Y. (2016). “Steady and unsteady pressure scour under bridges at clear-water conditions.” *Canadian Journal of Civil Engineering*, 43(4), 334–342.

Lagasse, P. F., Clopper, P. E., Zevenbergen, L. W., Spitz, W. J., Girard, L. G., Ayres Associates, Inc., and Fort Collins, CO. (2010). *Effects of debris on bridge pier scour*. Transportation Research Board, Washington, D.C.

Lyn, D. A. (2006). “Pressure-Flow Scour: A Re-Examination of the HEC-18 Equation.” *World Environmental and Water Resource Congress 2006*, Proceedings.

Lyn, D., Cooper, T., Yi, Y.-K., Sinha, R., and Rao, A. R. (2003). *Debris Accumulation at Bridge Crossings: Laboratory and Field Studies*. Purdue University, West Lafayette, IN.

May, R. W. P., Ackers, J. C., and Kirby, A. M. (2002). *Manual on scour at bridges and other hydraulic structures*. CIRIA C, CIRIA, London.

McKibbins et al. (2006). *Masonry arch bridges: condition appraisal and remedial treatment (Vol. C656)*.

Melbourne, C., Wang, J., and Tomor, A. K. (2007). “A new masonry arch bridge assessment strategy (SMART).” *Proceedings of the Institution of Civil Engineers-Bridge Engineering*, Thomas Telford, London.

Melville. (1997). “Pier and Abutment Scour: Integrated Approach.” *Journal of Hydraulic Engineering*, 123(2), 125–136.

Melville, B. W. (1992). “Local Scour at Bridge Abutments.” *Journal of Hydraulic Engineering*, 118(4), 615–631.

Melville, B. W. (2014). “Pressure-flow scour at bridges.” *Proceedings of the 7th International Conference on Scour and Erosion*, Perth, Australia.

Melville, B. W., and Chiew, Y.-M. (1999). “Time Scale for Local Scour at Bridge Piers.” *Journal of Hydraulic Engineering*, 125(1), 59–65.

Melville, B. W., and Coleman, S. E. (2000). *Bridge Scour*. Water Resources Publication.

Oliveira, D. V., Lourenço, P. B., and Lemos, C. (2010). “Geometric issues and ultimate load capacity of masonry arch bridges from the northwest Iberian Peninsula.” *Engineering Structures*, 32(12), 3955–3965.

Pagliara, S., and Carnacina, I. (2010). “Temporal scour evolution at bridge piers: effect of wood debris roughness and porosity.” *Journal of Hydraulic Research*, 48(1), 3–13.

Pagliara, S., and Carnacina, I. (2011). “Influence of Wood Debris Accumulation on Bridge Pier Scour.” *Journal of Hydraulic Engineering*, 137(2), 254–261.

Panici, D., and de Almeida, G. A. M. (2017). “Understanding the Formation of Woody Debris Jams at Bridge Piers.” IAHR, Kuala Lumpur.

Parola, A. C., Hagerty, D. J., Mueller, D. S., Melville, B. W., Parker, G., and Usher, J. S. (1997). “The Need for Research on Scour at Bridge Crossings.” ASCE, 1020–1020.

Proske, D., and van Gelder, P. (2009). *Safety of historical stone arch bridges*. Springer Science & Business Media.

Proske, D., Krawtschuk, A., Zeman, O., Scheidl, C., and Chiari, M. (2017). “Debris flow impacts on masonry arch bridges.” *Proceedings of the Institution of Civil Engineers - Bridge Engineering*, 1–12.

Raudkivi, A. J., and Ettema. (1983). “Clear-Water Scour at Cylindrical Piers.” *Journal of Hydraulic Engineering*, 109(3), 338–350.

Richardson, E. V., and Davies, S. R. (2001). *Evaluating Scour at Bridges.pdf*.

Richardson, E. V., Harrison, L. J., Richardson, J. R., and Davis, S. R. (1993). “Evaluating scour at bridges. Second edition.”

Richardson, J. E., and Panchang, V. G. (1998). “Three-Dimensional Simulation of Scour-Inducing Flow at Bridge Piers.” *Journal of Hydraulic Engineering*, 124(5), 530–540.

Robinson, J. (2000). “Analysis and assessment of masonry arch bridges.” PhD thesis, University of Edinburgh.

Sarhosis, V., Santis, S. D., and Felice, G. de. (2016). “A review of experimental investigations and assessment methods for masonry arch bridges.” *Structure and Infrastructure Engineering*, 12(11), 1439–1464.

Sheppard, D. M., Melville, B. W., and Demir. (2014). “Evaluation of Existing Equations for Local Scour at Bridge Piers.” *Journal of Hydraulic Engineering*, 140(1), 14–23.

Sutherland, A. J. (1986). *Reports on bridge failure.* RRU Occasional Paper, National Roads Board, Wellington, New Zealand.

Toth, E. (2015). “Asymmetric Error Functions for Reducing the Underestimation of Local Scour around Bridge Piers: Application to Neural Networks Models.” *Journal of Hydraulic Engineering*, 141(7), 04015011.

Umbrell, E. R., Young, G. K., Stein, S. M., and Jones, J. S. (1998). “Clear-Water Contraction Scour under Bridges in Pressure Flow.” *Journal of Hydraulic Engineering*, 124(2), 236–240.

Yalin, M. S. (1972). *Mechanics of sediment transport*. Pergamon Press.

Yalin, M. S., and da Silva, A. M. F. da. (2001). *Fluvial processes*. IAHR.